of the manuscript and suggestions. Additionally, the author thanks Patty Jasma, A. A. Osman, Lesley Varney, and Maggie Klonowska for technical assistance. The work was supported by an award from the University of Arizona, Center for Insect Science to X.J.S., grants to I.A.M. (NIH EY-03592, NSERC OPG 0000065), to L.P.T. and J.G.H. (NIH NS-28495), and to J.G.H. (NIH AI-23253).

[10] Construction of Line-Scan Confocal Microscope for Physiological Recording

By NICK CALLAMARAS and IAN PARKER

Introduction

The use of confocal laser scanning microscopes (CLSM) together with fluorescent Ca^{2+} indicator dyes allows detailed imaging studies of the spatio-temporal aspects of intracellular Ca^{2+} signaling. For example, the high spatial and temporal resolution of this technique has revealed that release of Ca^{2+} from intracellular organelles into the cytosol occurs as transient, elementary signals, arising at specific subcellular release sites. These elementary events include Ca^{2+} "puffs" mediated through inositol 1,4,5-trisphosphate ($InsP_3$) receptors in *Xenopus* oocytes and HeLa cells[1–4] and Ca^{2+} "sparks" mediated through ryanodine receptors in cardiac muscle.[5] This article describes the construction and performance of a CLSM, combined with a UV illumination system for the photolysis of caged compounds, presently in use in the authors' laboratory for studies of $InsP_3$-mediated intracellular Ca^{2+} release in *Xenopus* oocytes. This system can be adapted readily to virtually any inverted microscope and offers greater versatility and equal or better performance than comparable commercial instruments for a fraction of the cost.

Commercial confocal microscopes fall broadly into two classes: those designed for morphological studies of fixed or slowly changing specimens and video-rate (30 Hz) full-field imaging systems for monitoring dynamic cellular signals. In either case, the application of these instruments for physiological studies often presents several difficulties. First, design constraints in commercial instruments tend to complicate the optical paths,

[1] I. Parker and Y. Yao, *Proc. R. Soc. (Lond.) B. Biol. Sci.* **246,** 269 (1991).
[2] Y. Yao, J. Choi, and I. Parker, *J. Physiol. (Lond.)* **482,** 533 (1995).
[3] M. Bootman, E. Niggli, M. Berridge, and P. Lipp, *J. Physiol. (Lond.)* **499,** 307 (1997).
[4] X.-P. Sun, N. Callamaras, and I. Parker, *J. Physiol. (Lond.)* **509,** 67 (1998).
[5] H. Cheng, W. J. Lederer, and M. B. Cannell, *Science* **262,** 740 (1993).

0076-6879/99 $30.00

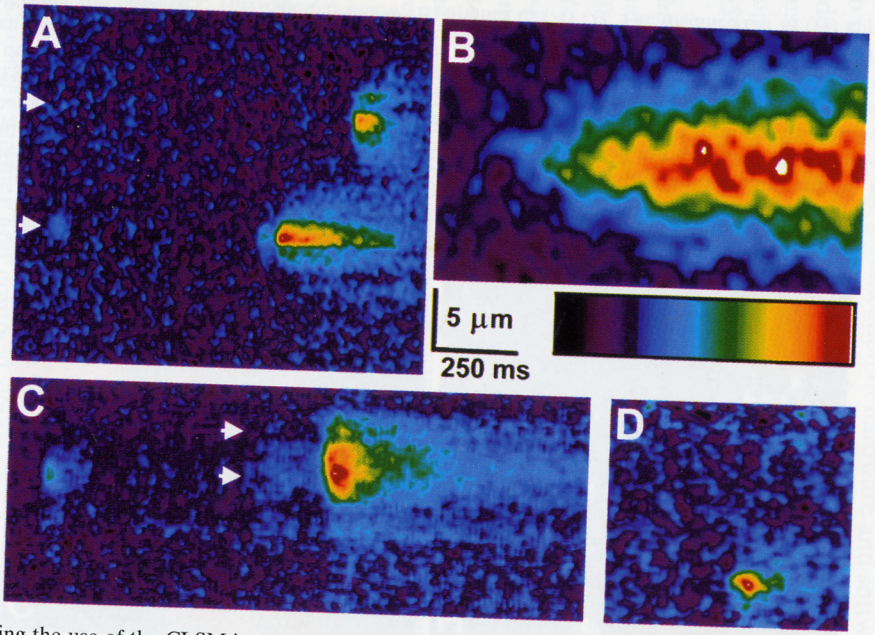

FIG. 8. Images illustrating the use of the CLSM in various modes. (A) Line-scan images of elementary events in the *Xenopus* oocyte. Events were evoked by the photorelease of $InsP_3$ by a photolysis flash delivered before the start of the image and recorded at 8 msec per scan line. Small events (see lower arrow) may represent Ca^{2+} flux through a single channel. Color bar indicates F/F_0 from 0.9 to 2.2. (B) High-resolution line-scan image of the rising phase of a calcium release event (puff). Image shows an average of five sharply focal puffs recorded at a resolution of 1.5 msec per line and 0.2 μm per pixel and formed by aligning, in time and space, the first detectable rise in fluorescence during individual events. Color bar indicates F/F_0 from 0.9 to 2.2. (C and D) Radial distribution of calcium puffs evoked by photorelease of $InsP_3$ before each record. Images were obtained by fast axial scanning and show distance into the oocyte running downward and time from left to right. Color bar indicates F/F_0 from 0.9 to 2.9.

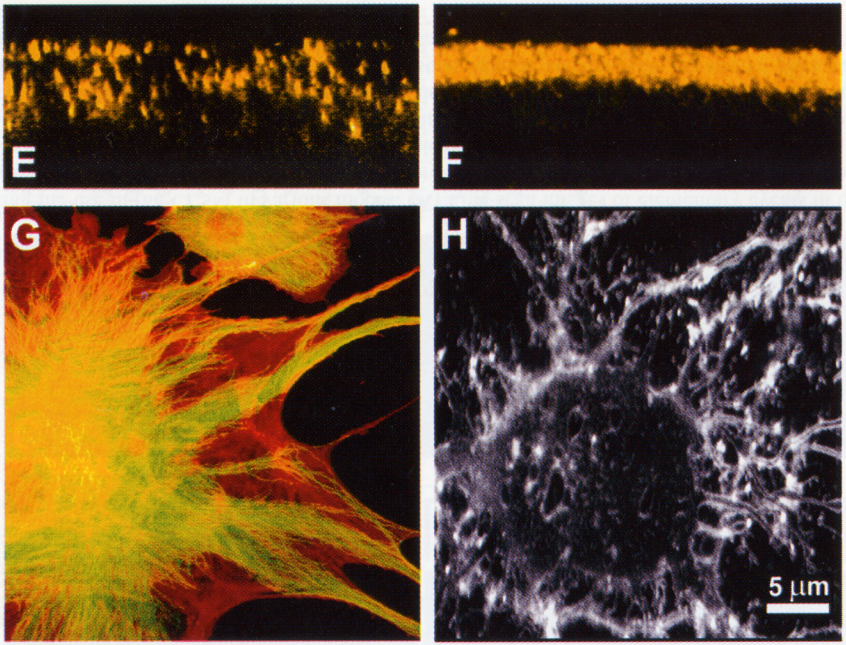

FIG. 8. (*continued*). (E and F) Radial distribution of $InsP_3$ receptors in the oocyte. The pseudo-colored image in (E) is an x–z scan into the vegetal hemisphere of an intact oocyte showing a punctate distribution of $InsP_3Rs$. Image in (F) shows the more dense distribution of $InsP_3$ receptors in the animal hemisphere obtained by x–y scanning of a physically sectioned oocyte. $InsP_3Rs$ were visualized with a polyclonal antibody to the $InsP_3R_1$ and Cy3-conjugated secondary antibody. The plasma membrane of the cell is aligned near the upper edge of the image; the vertical axis represents depth into the cell (z axis) and the horizontal axis lateral (y) position. (G) Pseudo-colored image of endothelial cells stained for tubulin (green) and F-actin (red). (H) Gray-scale images of cultured cortical neurons stained with Di8-ANNEPS to visualize surface membranes, showing cell soma and processes. The scale bar below (B) applies to (A–D). The distance bar in (H) applies to (E–H). All images were obtained with an Olympus 40× fluor objective; NA, 1.35.

and the detectors and associated electronics are often relatively inefficient.[6] These factors lead to a low overall efficiency in the detection of emitted photons, requiring the use of a high laser intensity and/or a large confocal aperture to obtain images with an adequate signal-to-noise ratio. Second, the "black box" approach of proprietary commercial systems discourages, if not prohibits, the modification of hardware and software often necessary to optimize the device for a specific application. For example, swapping or adding lasers and filters to optimize the fluorescence of a specific dye or customizing software routines for data acquisition and analysis may be constrained severely. Moreover, the high cost of systems (typically >$125,000) makes them difficult to justify by individual investigators.

To overcome these limitations, we constructed a combined CLSM/UV photolysis system with the following advantages: (1) a simple optical path that, together with an avalanche photodiode detector with high quantum efficiency, provides a high efficiency of detection; (2) true photon-counting circuitry and associated software that allows complete flexibility for data acquisition and analysis; (3) access to and control of hardware and software components, allowing great flexibility in the choice of wavelengths, scan rate and length, and data acquisition and processing; and (4) affordability. The total cost to add confocal scanning capability to an existing inverted microscope is <$20,000.

In practice, this system has proven to be a powerful and flexible tool for the study of $InsP_3$-mediated Ca^{2+} release in *Xenopus* oocytes and cardiac myocytes.[7,8] Although this system was designed primarily for rapid (up to 1 kHz) line-scan imaging of Ca^{2+} puffs and sparks, it also works well for many other applications, including high-resolution morphological studies.

Design and Construction of CLSM

Overview

The optical system described in this article consists of two independent units: a laser scanner and confocal detector comprising the CLSM and a UV photolysis system. These are mounted on a 4 × 2.5-ft optical breadboard (Melles Griot, Irvine, CA) and are interfaced to an Olympus IX70 inverted microscope through the video and epifluorescence ports of the microscope,

[6] J. B. Pawley, *in* "Handbook of Biological and Confocal Microscopy" (J. B. Pawley, ed.). Plenum Press, New York, 1995.
[7] N. Callamaras, J. Marchant, X.-P. Sun, and I. Parker, *J. Physiol.* (*Lond.*) **509.1,** 81 (1998).
[8] I. Parker and W. G. Wier, *J. Physiol.* (*Lond.*) **505,** 337 (1997).

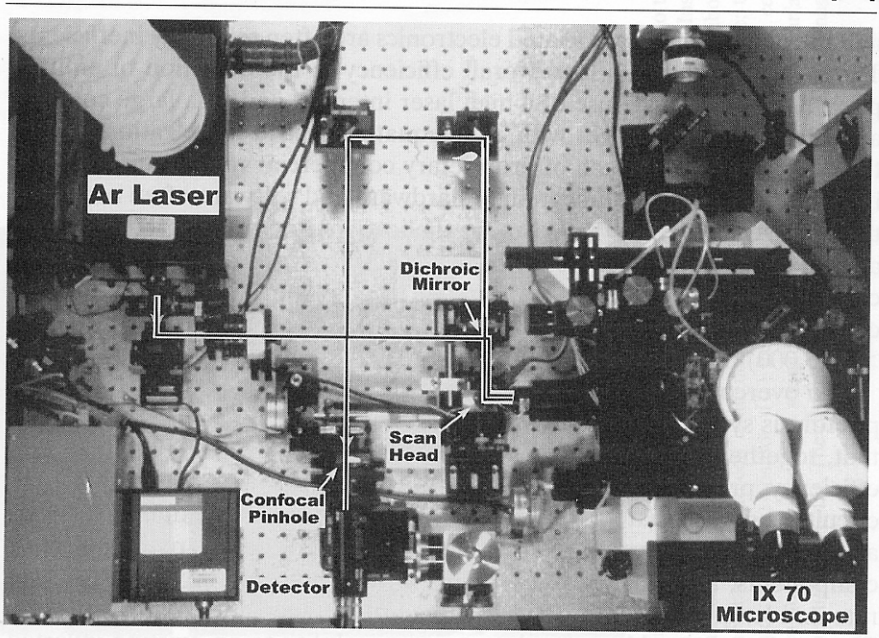

FIG. 1. Overhead photograph of the CLSM after removal of the cover.

respectively (Fig. 1). To maximize light throughput, all mirror and lens surfaces are broadband dielectric coated, and covers over the optical path (especially between the confocal aperture and the detector) are employed to reduce stray light.

At the heart of the CLSM is a photon-counting module (SPCM-AQ-121; EG&G Optoelectronics Inc., Vaudreuil, Canada) that comes complete with an avalanche photodiode, pulse discriminator, cooling circuitry, high-voltage power supply, and an external 5-V power supply. This unit provides a greater photon detection probability (>40% between 500 and 700 nm) than achieved by prismatic-face photomultiplier tubes,[9] while possessing similar dark count rates. Output from the module is TTL pulses (5 nsec duration), with the output rate proportional linearly (<10% deviation) to light intensity for count rates up to 2 MHz and saturating above 15 MHz. In addition, the small active area of the detector (200 μm) rejects stray light greatly, making it possible to operate the microscope under normal room lights.

The following sections describe the construction and use of this system. For simplicity, the instrument is described as set up for use with fluorophores

[9] A. MacGregor, *in* "Photonics Design and Applications Handbook" H 111, 1993.

with spectra similar to fluorescein. For details pertaining to the electronics and drive circuitry, as well as tips on aligning optical paths, see Parker *et al.*[10] Copies of circuit diagrams and software routines are available from the authors on request.

Fluorescence Excitation Path

Figure 2A shows the schematic layout of the CLSM optics. Fluorescence excitation is derived from a 100-mW multiline argon ion laser (Omnichrome, Chino, CA), bolted to the optical breadboard using insulating plastic brackets to raise the beam height to the axis of the video port on the microscope. Because the output from the laser far exceeds that required (typically <100 μW at the specimen), the laser is run in "standby" mode to prolong the life of the laser tube. After passing through an electronically controlled shutter (S1), allowing blocking of the beam between recordings, the beam is steered by mirror (M1) through a narrow-band interference filter (F1) selecting the 488-nm emission line. A rotating polarizer (P) allows a continually variable attenuation of the polarized laser light over a >100-fold range, and additional neutral density filters are placed in the light path as needed. The laser beam is then expanded by lens L1 ($f = -10$ cm) to overfill the back aperture of the microscope objective and is reflected by a dichroic mirror (DM; λ 500 nm, Omega Optical, Brattleboro, VT, mounted in a Nikon filter cube) onto a galvanometer-driven scan mirror in the confocal scan head. This mirror is mounted at a conjugate telecentric plane, formed by a scan lens (L2), consisting of a wide-field 10× eyepiece (Zeiss) mounted to the bayonet adapter of the video port. The beam diameter at the scan mirror is about 2 mm, allowing use of a small mirror (3 mm square), with low inertia, permitting fast scan rates. Rotations of the scan mirror result in deflections in position of the diffraction-limited laser spot focused in the specimen by the microscope objective. The maximum deflection in our system is limited by the aperture of L2 and corresponds to about two-thirds of the field viewed through the microscope oculars or about 200 μm with a 40× objective. Recordings were made with a 40× oil-immersion fluorescence objective (1.35 NA) with good UV transmission to maximize confocal sectioning ability and allow simultaneous photolysis of caged compounds.

Fluorescence Emission Path

Fluorescence emission is collected by the objective and passed back through the video port. Because the ability to directly view fluorescence

[10] I. Parker, N. Callamaras, and W. Wier, *Cell Calcium* **21,** 441 (1997).

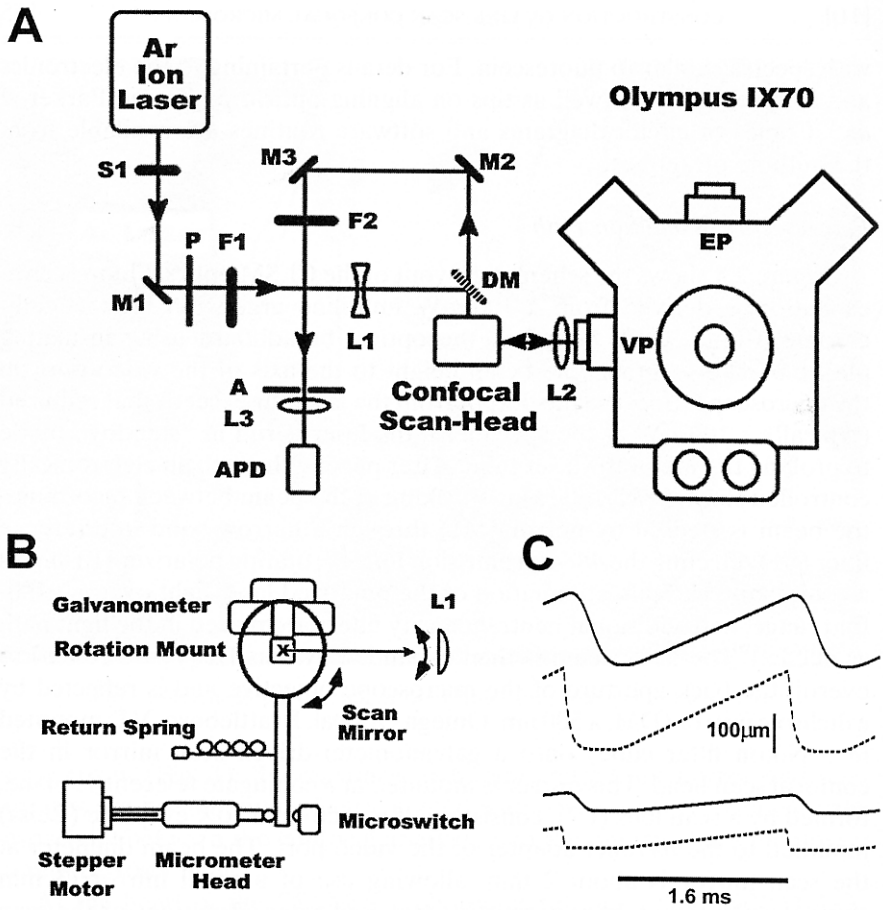

FIG. 2. Optical layout of the CLSM and drive waveforms. (A) The CLSM is interfaced through the video port (VP) on the left of the Olympus IX70 microscope. S1, shutter; M1–3, fully reflecting front surface mirrors; P, rotating polarizer (variable attenuator); F1, 488-nm narrow-band interference filter; L1, diverging lens, focal length = −10 cm; DM, dichroic mirror, λ = 500 nm; L2, scan lens (Zeiss 10× wide-field eyepiece); F2, barrier filter (515-nm long-pass color glass: Schott OG515); A, confocal aperture; L3, converging lens, f = 5 cm; APD, avalanche photodiode module. (B) Diagram of the scan head looking from the front of the microscope. The x-scan galvanometer is mounted through a metal block (serving also as a heat sink) to a stage allowing rotation around the axis marked by the cross. A lever attached to the stage is driven by a motorized micrometer to rotate the scan mirror in the y axis (vertical), while the galvanometer allows simultaneous fast scanning in the x axis (horizontal). Alignment of repeated scans is achieved by a microswitch, contacted at a preset position, that gates data acquisition. (C) Fidelity of mirror scan. Traces show ramp drive waveforms (dashed curves) and actual mirror position (solid curves) for small (lower) and large (upper) scan displacements, both at a scan rate of 2 msec per line. With a 40× objective, the galvanometer deflections correspond to 50- and 200-μm scan lengths, respectively. The horizontal bar indicates the linear ramp time during which image data are acquired. The flyback interval was set to 400 μsec.

excited by the laser scan line during experiments is of great assistance, the microscope is equipped with an 80/20 beam splitter directing light to the video port and oculars, respectively. The loss of 20% of the excitation light can easily be compensated for by increasing laser power. Some manufacturers (e.g., Nikon Inc., Melville, NY) obviate this minor difficulty by equipping their inverted microscopes with both 80/20 and 100/0 beam splitters. For safety while viewing, a 510-nm long-pass filter is installed before the microscope oculars to block 488-nm laser light. Fluorescence light passing through L2 is descanned by the galvanometer mirror so that a stationary beam passes through the dichroic mirror and is deflected by mirrors M2 and M3 onto the detector system (Fig. 2A). The purpose of M2 and M3 is to provide a longer optical path so that a highly magnified (about $\times 1000$) image of the fluorescent spot is formed at the plane occupied by the confocal aperture A, and the z-axis resolution of the system can be optimized by varying the size of this pinhole. Because of the high magnification, the required apertures are relatively large (0.5–2 mm), and a range of sizes were made using a broken glass microelectrode to punch holes in pieces of aluminum foil.

F2 is a sharp cutoff 510-nm long-pass filter, which blocks the 488-nm laser light while transmitting fluorescence at $\lambda > 510$ nm. Use of a long-pass filter maximizes detection efficiency, but for some purposes, a broad band-pass filter provides better rejection of stray light and autofluorescence at wavelengths away from the emission maximum of the fluorophore. Finally, the light passing through the aperture is focused by lens L3 ($f = 5$ cm) to a small spot centered within the active area of the avalanche photodiode detector, which, to assist in alignment, is mounted on a low-profile micropositioner (New Focus Inc., Santa Clara, CA).

Scan Head

Fast x-scanning of the confocal spot is achieved by a galvanometer-based mirror positioning system (Model 6800/CB6588; Cambridge Technology, Inc., Watertown, MA), which is mounted in the scan head assembly to scan the laser beam in the horizontal (x) plane (Fig. 2B). For correct operation, it is critical that the axis of the mirror is positioned at the conjugate telecentric plane imaged by the scan lens L2 and that the galvanometer be oriented so light is reflected by the front surface of the mirror. Correct alignment can be determined by placing a piece of frosted glass over an open position on the microscope nosepiece. When adjusted correctly, the glass should be illuminated uniformly and the laser light stable as the mirror is scanned. A practical point is to mount the galvanometer in a holder that

acts as a heat sink, as the drive coil generates appreciable heat at high scan rates.

To permit two-dimensional (x–y) scans, the galvanometer is mounted on a rotation stage (prism mount; New Focus Inc.) allowing simultaneous rotation around a horizontal axis orthogonal to and passing through the center of the scan mirror (Fig. 2B). An arm attached to the stage is driven by a micrometer and stepper motor, allowing vertical deflection of the laser beam in the y axis at a precise rate determined by the pulse rate of the stepper motor controller. To obtain square pixels at various "zoom" settings, the motor speed settings are calibrated for a range of commonly used line lengths and scan rates. Use of a single mirror scanned around two orthogonal axes, rather than a dual-mirror system, simplifies the optical path, minimizing light loss and problems of alignment, although it does limit the maximum acquisition rate of x–y images to about 1 frame every 2 sec.

The galvanometer scanner is driven by a servo amplifier, such that the ramp drive signal derived from the electronics unit described later produces a linear change in scan angle and hence linear displacement of the confocal spot. During experiments, it is convenient to monitor the analog signal from the detector using an oscilloscope to provide immediate visual feedback, e.g., to locate sites of Ca^{2+} release as the specimen is moved using the mechanical stage of the microscope. Figure 2C illustrates ramp waveforms (at a scan rate of 2 msec per line) and the corresponding mirror positions reported by the optical position sensor on the galvanometer.

Electronics

A custom electronics unit was designed to both process output from the detector and provide a ramp drive signal for the galvanometer driving the x-scan mirror (Fig. 3). This is driven by a pixel clock, generating pulses at switch-selected intervals between 1 μsec and 1 msec. During each pixel interval, photon counts from the detector are summed by an 8-bit counter. Following the next clock pulse, this sum, representing the pixel intensity, is made available on both digital or analog interfaces for sampling by a computer, and the counter is reset to zero to begin counting again. An LED provides visual warning if the pixel counts exceed the maximum count of 255. The pixel clock also drives the ramp generator used to drive the scan mirror. Pixel pulses are summed by a 10-bit counter, the output of which is fed continuously through an analog-to-digital converter to produce a linear stepwise ramp. A thumbwheel switch is used to set the desired number of pixels per scan line (1–999), and when this count is reached, the counter is reset to zero, a TTL pulse is sent to a "line sync" output

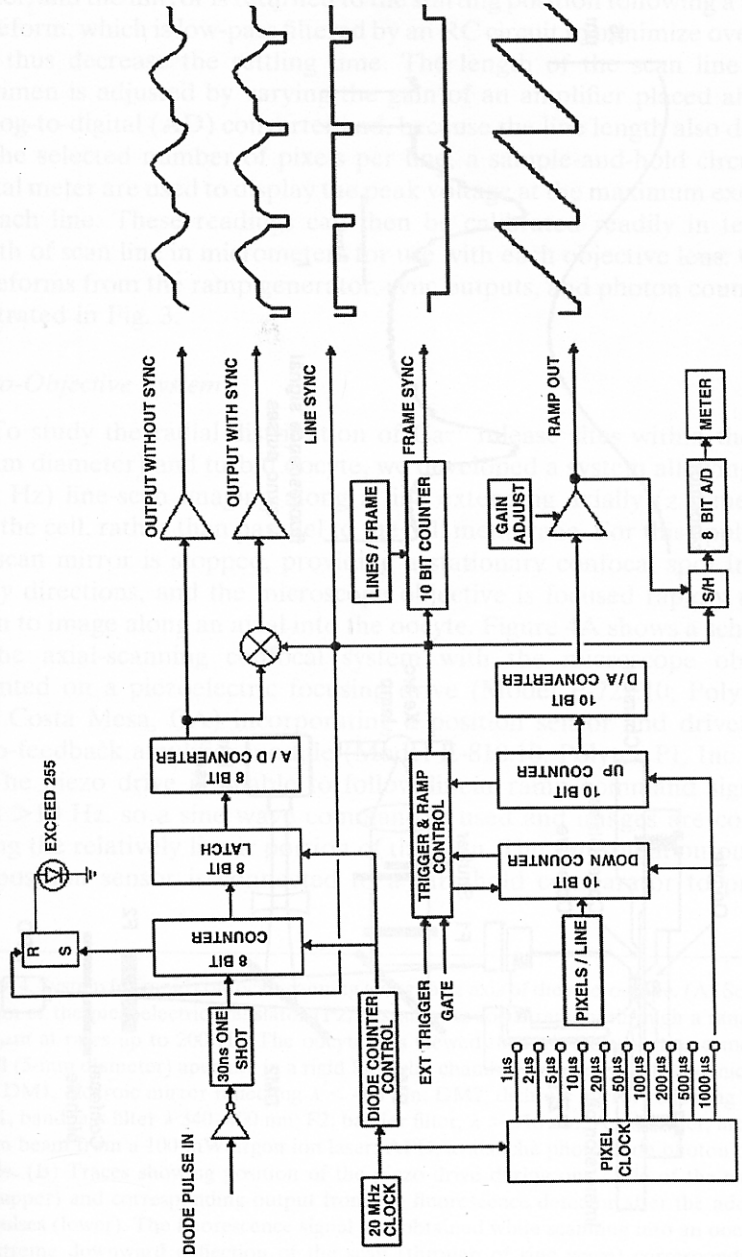

FIG. 3. Block diagram of the mirror controller/photon counting unit and resulting output waveforms. See text for details.

socket, and the mirror is returned to the starting position following a flyback waveform, which is low-pass filtered by an RC circuit to minimize overshoot and thus decrease the settling time. The length of the scan line in the specimen is adjusted by varying the gain of an amplifier placed after the analog-to-digital (AD) converter and, because the line length also depends on the selected number of pixels per line, a sample-and-hold circuit and digital meter are used to display the peak voltage at the maximum excursion of each line. These readings can then be calibrated readily in terms of length of scan line in micrometers for use with each objective lens. Output waveforms from the ramp generator, sync outputs, and photon counter are illustrated in Fig. 3.

Piezo-Objective System

To study the radial distribution of Ca^{2+} release sites within the large (1 mm diameter) and turbid oocyte, we developed a system allowing rapid (100 Hz) line-scan imaging along a line extending axially (z dimension) into the cell, rather than parallel to the cell membrane. For this application the scan mirror is stopped, providing a stationary confocal spot in the x and y directions, and the microscope objective is focused rapidly up and down to image along an axial into the oocyte. Figure 4A shows a schematic of the axial-scanning confocal system with the microscope objective mounted on a piezoelectric focusing drive (Model P-721.10; Polytec PI, Inc., Costa Mesa, CA) incorporating a position sensor and driven by a servo-feedback amplifier module (Model E-810.10; Polytec PI, Inc.).

The piezo drive is unable to follow linear ramp command signals at rates >10 Hz, so a sine wave command is used and images are collected during the relatively linear portion of the scan. The sinusoidal output from the position sensor is connected to a threshold comparator to produce

FIG. 4. System for rapid confocal scanning along the z axis of the microscope. (A) Schematic diagram of the piezoelectric translator (PZT) system to focus rapidly through a range of up to 35 μm at rates up to 200 Hz. The oocyte was viewed through a cover glass cemented in a small (5-mm diameter) aperture in a rigid Plexiglas chamber bolted firmly to the microscope stage. DM1, dichroic mirror reflecting $\lambda < 400$ nm; DM2, dichroic mirror reflecting $\lambda < 500$ nm; F1, bandpass filter λ 340–400 nm; F2, barrier filter, $\lambda > 510$ nm; Ar ion laser, attenuated 488-nm beam from a 100-mW argon ion laser; APD, avalanche photodiode photon counting module. (B) Traces showing position of the piezo drive during one cycle of the sine-wave scan (upper) and corresponding output from the fluorescence detector after the addition of sync pulses (lower). The fluorescence signal was obtained while scanning into an oocyte, and the extreme downward deflection of the scan (through of sine wave) corresponds to the position of the cover glass. The fluorescence profiles on the "down" and "up" scans are not perfect mirror images because of lateral hysteresis in the translator.

synchronization pulses, which are then added to the continuous stream of fluorescence data from the confocal detector (Fig. 4B). Images are formed at a rate of 100 Hz, with integration times of 10 or 20 μsec per pixel and a peak-to-peak scan amplitude of about 32 μm, providing nominal pixel sizes of about 0.05 or 0.1 μm throughout the linear range of the scan.

A practical difficulty is that the oil-immersion objective transmits vibration to the specimen through the oil. To minimize this, the oocyte is imaged through a cover glass cemented to a small (5-mm diameter) aperture in the base of a rigid Plexiglas recording chamber that is bolted firmly onto the microscope stage (Fig. 4A). This rigid recording chamber allows recordings at rates of 100 Hz to be made without difficulty. Another concern is that lateral hysteresis of the piezo drive unit results in the upward scan imaging of a slightly different (<1 μm) region of the cell; therefore only data collected during the downward scan of each cycle are used to construct images.

Computer Software

The photon count output and line sync signal are combined, digitized as a gap-free continuous record using a Digidata 1200 interface and Axoscope software package (Axon Instruments, Foster City, CA), and stored directly on hard disk for durations limited only by the available disk space. Custom routines written using the IDL programming language (Research Systems Inc., Boulder, CO) are then used to construct and analyze images formed from the raw data files. In brief, a routine identifies the positions of line sync pulses in the data file and forms an image array in which successive columns represent successive line scans aligned by the rising edges of preceding sync pulses.

Photolysis System

To allow simultaneous confocal fluorescence imaging and photolysis of caged intracellular compounds, UV (<400 nm) light sources are interfaced through the epifluorescence port of the microscope in conjunction with a UV filter cube. Figure 5 shows the layout of the optical components and the photolysis light paths in our system. UV light is provided by a continuous arc lamp source and a pulsed UV laser, with light from both being combined by a 50% beam-splitting mirror. The choice of light source depends on the experimental requirements. For photorelease of caged compounds over wide areas (10–100 μm), UV light is derived from a 75-W xenon arc lamp mounted in a Zeiss housing and operated from a stabilized constant-current power supply. An electronic shutter (Uniblitz; Vincent Associates, NY)

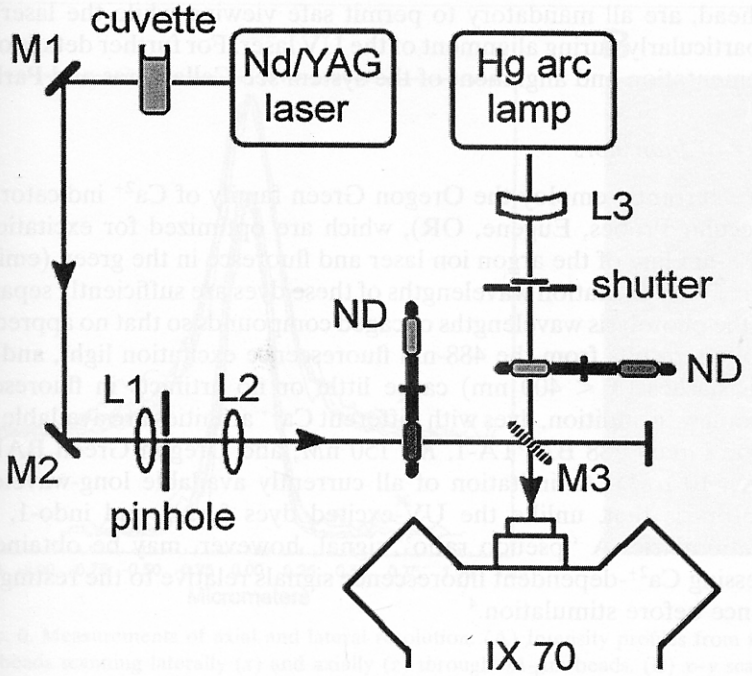

FIG. 5. Optical schematic of the systems for wide-field and point photolysis of caged $InsP_3$. See text for details.

controls exposure duration while a set of neutral density wheels (3.0 OD in steps of 0.1 OD, New Focus Inc.) allow control of light intensity.

For "point" photorelease, a laser system is employed, which consists of a Mini-Lite frequency-tripled (355 nm) Nd-YAG laser (Continuum, Santa Clara, CA) mounted on an optical table with insulating stand-offs to avoid electrical noise. The laser can be operated in single-shot mode (5-nsec pulse, triggered by a push switch or TTL input) or pulsed repeatedly at up to 10 Hz. A quartz cuvette containing a solution of $FeSO_4$ is used to initially attenuate the beam (which otherwise is sufficiently powerful to destroy mirror coatings) about 10-fold, and neutral density filter wheels provide further graded attenuation. Lenses L1 and L2 form a beam expander and spatial filter, so that the laser beam fills the back aperture of the objective lens, and can be focused to a near diffraction limited spot in the specimen. A beam dump is placed after M3 to prevent the beam passing into the room. Appropriate safety precautions, including laser safety goggles, a UV-blocking filter in the Olympus filter cube, and an additional long-pass filter ($\lambda > 510$ nm) inserted permanently in the microscope binoc-

ular head, are all mandatory to permit safe viewing while the laser is in use, particularly during alignment of the UV laser. For further details on the implementation and alignment of the system see Callamaras and Parker.[11]

Choice of Indicators

We currently employ the Oregon Green family of Ca^{2+} indicator dyes (Molecular Probes, Eugene, OR), which are optimized for excitation by the 488-nm line of the argon ion laser and fluoresce in the green (emission 520 nm). The excitation wavelengths of these dyes are sufficiently separated from the photolysis wavelengths of caged compounds so that no appreciable photolysis results from the 488-nm fluorescence excitation light, and photolysis flashes ($\lambda < 400$ nm) cause little or no artifacts in fluorescence recordings. In addition, dyes with different Ca^{2+} affinities are available (e.g., Oregon Green 488 BAPTA-1, K_D 150 nM; and Oregon Green BAPTA-5N, K_D 10 μM). A limitation of all currently available long-wavelength indicators is that, unlike the UV-excited dyes fura-2 and indo-1, none are ratiometric. A "pseudo ratio" signal, however, may be obtained by expressing Ca^{2+}-dependent fluorescence signals relative to the resting fluorescence before stimulation.[4]

Performance of CLSM System

Spatial Resolution

Various approaches may be used to characterize the lateral and axial (z axis) resolution of a confocal microscope. A simple test of z-axis resolution is to measure reflected light from a stationary laser spot while the microscope is focused through a front-surface mirror.[6] This technique yields the full-width at half-maximum intensity (FWHM), a number that can be compared with other systems and aids in aligning the system. Measurement of the normalized reflected intensity as the microscope was focused through a mirrored slide, using various confocal apertures, showed that the FWHM decreases with decreasing size of the aperture and reduces to about 500 nm with an aperture of 0.75 mm diameter.[10] A more physiologically relevant test was made by imaging fluorescent latex beads (green fluorescent latex microspheres: Molecular Probes Inc.) in aqueous medium. Figure 6A shows intensity profiles from axial (x–z) and lateral (x–y) scans through the center of subresolution (0.1 μm) beads, providing measures of the point-spread function of the CLSM. The FWHM of the axial and lateral point-spread

[11] N. Callamaras and I. Parker, *Methods Enzymol.* **291,** 497 (1998).

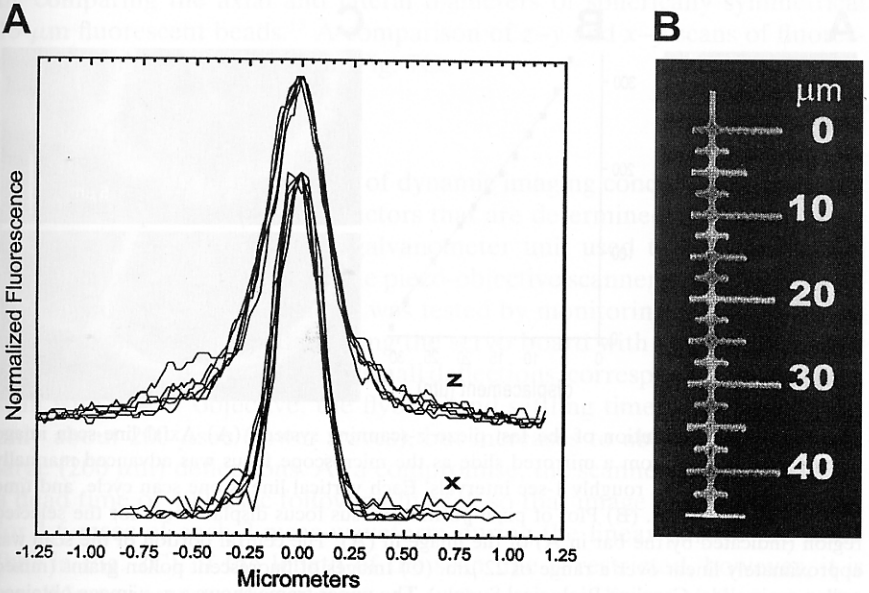

FIG. 6. Measurements of axial and lateral resolution. (A) Intensity profiles from images of six beads scanning laterally (x) and axially (z) through 0.1-μm beads. (B) x–y scan of a mirrored micrometer calibration slide. All images were obtained with an Olympus 40× fluor objective; NA, 1.35.

functions are about 300 and 400 nm, respectively, with no correction applied for the finite size of the beads. Finally, the linearity of the overall scanning system (including both the galvanometer and optics) was tested by imaging (in reflectance mode) a mirrored micrometer calibration slide (Fig. 6B). Any deviations from linearity in the image of this graticule were <500 nm over a 50-μm scan line (i.e., <1%). A similar performance was also achieved for scans in the y axis. Therefore, when aligned properly, the spatial resolution of the CLSM is close to the diffraction-limited performance expected for a confocal microscope,[12] and the user has complete control over the desired pixel resolution (e.g., up to 1000 × 2000 pixels in x–y scan mode).

To calibrate the distance scale and linearity of axial-scan images, reflected laser light was monitored from a mirrored slide after removing the barrier filter (F2; Fig. 2A), resulting in a sharp peak of reflected laser light as the microscope focus knob was advanced manually in 2-μm increments

[12] S. Inoue, *in* "Handbook of Biological and Confocal Microscopy" (J. B. Pawley, ed.). Plenum Press, New York, 1995.

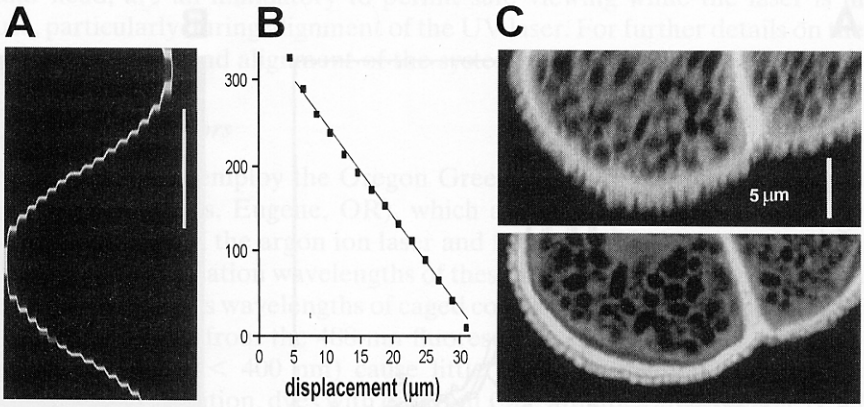

FIG. 7. Axial resolution of the fast piezo z-scanning system. (A) Axial line-scan image showing reflectance from a mirrored slide as the microscope focus was advanced manually in 2-μm increments at roughly 1-sec intervals. Each vertical line is one scan cycle, and time runs from left to right. (B) Plot of pixel position versus focus displacement for the selected region (indicated by the bar in A) of the image in (A). The central portion of the scan was approximately linear over a range of 22 μm. (C) Images of fluorescent pollen grains (mixed pollen grain slide; Carolina Biological Supply). The upper frame shows a z–y image obtained using the piezo drive to scan rapidly (100 Hz) in the z axis (depicted vertically), while the laser spot was scanned slowly in the y axis by a rotating mirror. For comparison, the lower frame shows a conventional lateral x–y scan of a matching region of a different pollen grain. All images were obtained with an Olympus 40× fluor objective; NA, 1.35.

to move the mirror through the entire scan range of the objective (Fig. 7A). Steps in the image thus correspond to 2-μm displacements of the objective lens, and the distance scale of the image could be calibrated by plotting the pixel position of peak reflectance against displacement of the microscope nosepiece. Figure 7B shows a plot of pixel position of peak reflectance against displacement of the objective over the region marked by the bar in Fig. 7C. With the system set to give a peak-to-peak displacement of 32 μm, a linear range of >20 μm was obtained around the center of the scan. The image in the upper trace shows a z–y image obtained with the piezo scanned rapidly (100 Hz) in the z axis while the laser spot was scanned in the y axis by rotating the scan head, whereas the lower trace shows an x–y image of a similar pollen grain.

A consideration in axial imaging is the refractive index mismatch among water, the cover glass, and immersion oil resulting in a change in focal distance in the specimen that is slightly less than the corresponding movement of the objective. To correct for this effect, measurements based on the physical position of the objective were scaled by dividing by an experimentally derived factor of 1.17, arrived at by focusing on the advancing tip of a microelectrode in water using a calibrated manipulator, and confirmed

by comparing the axial and lateral diameters of spherically symmetrical 15-μm fluorescent beads.[13] A comparison of z–y and x–y scans of fluorescent pollen grains is shown in Fig. 7C.

Temporal Resolution

Other aspects of the fidelity of dynamic imaging concern the maximum possible temporal resolution; factors that are determined primarily by the mechanical properties of the galvanometer unit used to rotate the scan mirror (in x-scan mode) or by the piezo-objective scanner (in z-scan mode). The speed of the galvanometer was tested by monitoring the output from the position encoder while driving the servo board with rapid (2 msec per line) ramp signals (Fig. 2C). For small deflections, corresponding to a 50-μm scan with a 40× objective, the flyback and settling time after each line is only about 200 μsec (lower traces), but increases to about 400 μsec with large (200 μm) deflections. As a compromise, the scanner is operated with a dead time of 400 μsec following flyback so that image data are collected for 1.6 msec of each 2-msec waveform during the linear part of the ramp (bar in Fig. 2C). If the length of the scan line is restricted, however, it is possible to increase the scan speed to 1 msec per line and decrease the dead time to 200 μsec to collect data for 800 μsec each scan. In addition, line-scan data can be recorded continuously, unlike some commercial instruments that impose gaps after 512 or 1024 lines. This allows the activity of individual Ca^{2+} release sites to be monitored for prolonged periods and has revealed that individual sites may undergo long-term changes in "mode" or frequency of response.[8] When acquiring x–y images, a 1000 × 1000 pixel image (250 μm with 40× objective) takes about 21 sec to acquire using a pixel dwell time of 20 μsec. Images with lower resolution can be acquired with correspondingly shorter scan times. When acquiring axial line-scan (z–t) images the piezo drive could follow a sine-wave command signal at rates up to 200 Hz with a maximum excursion of about 35 μm. This response time is sufficiently rapid that it should be possible to use the piezo drive in conjunction with commercially available video-rate confocal microscopes so as to obtain x–z images at frame rates as fast as 60 Hz.

Applications

Imaging of Local Ca^{2+} Transients

The confocal scanner was designed primarily for the line-scan confocal recording of localized transient intracellular Ca^{2+} signals: $InsP_3$-mediated

[13] N. Callamaras and I. Parker, *J. Gen. Physiol.* **113,** 199 (1999).

puffs in *Xenopus* oocytes[14] and sparks in cardiac cells.[5,15] These events have rapid (tens or a few hundred millisecond) time courses and involve Ca^{2+} signals localized to within a few micrometers. Thus, imaging systems with high spatial and temporal resolution are required, and the use of confocal microscopy provides a particular advantage by avoiding blurring and out-of-focus fluorescence. Figures 8A and 8B (see color insert) illustrate Ca^{2+} puffs evoked in an oocyte by photoreleasing $InsP_3$ throughout a roughly 100-μm spot around the scan line using a flash of UV light provided by the arc lamp system shown in Fig. 5. Two puffs arising independently at sites about 10 μm apart are shown in Fig. 8A (see arrows). In addition, yet smaller "blips" can be observed occurring about 500 ms before and just preceding the lower puff in Fig. 8A. Such events were too small to resolve previously in video-rate confocal images obtained using a Noran Odyssey system[14] and probably represent Ca^{2+} flux through individual ion channels. For this application, a scan rate of 8 msec per line provided sufficient resolution of the time course of puffs; four times faster than the frame rate of a conventional video system. The image in Fig. 8B shows the average of five sharply focal puffs recorded at a faster temporal resolution (1.5 msec per line). The beginning of this image shows that the release of Ca^{2+} arises from a virtual point source of approximately 0.25 μm (at or below the limit of resolution of the system).

$InsP_3$-sensitive release sites in the oocyte are distributed irregularly in the x–y axes (i.e., parallel to the surface membrane) at a mean spacing of a few micrometers,[7,14] but little is known about their radial distribution. The piezoelectric objective scanning system described here provided a means to obtain time-resolved confocal images of transient Ca^{2+} release events along an axis running into the oocyte. Figures 8C and 8D illustrate Ca^{2+} puffs at varying depths in the oocyte evoked by brief photorelease of $InsP_3$. Figure 8C (see color insert) shows differentially activated, yet closely adjacent, sites whereas Figure 8D (see color insert) shows activation of a relatively deep site. Studies using this technique have revealed that puffs arise largely from release sites distributed in a thin (6 μm), superficial band a few micrometers below the cell surface.[13]

Using CLSM for Morphological Studies

Although the confocal scanner was built primarily for fast line-scan imaging of Ca^{2+} transients, it also works well for morphological studies using x–y and x–z scanning at slow frame rates, as shown in Figs. 8E–8H (see color inserts). The optical sectioning ability of the CLSM was used to

[14] I. Parker, J. Choi, and Y. Yao, *Cell Calcium* **20,** 105 (1996).
[15] J. R. Lopez-Lopez, P. S. Shacklock, C. W. Balke, and W. G. Wier, *Science* **268,** 1042 (1995).

localize $InsP_3R$ antibody staining in unsectioned intact oocytes (Fig. 8E, see color insert) to correlate with the distribution of functional release sites in a thin subplasmalemmal band. Receptor staining is visualized in an x–z image of the vegetal hemisphere, made by slowly advancing the focus knob of the microscope with a synchronous motor. In the vegetal hemisphere, a sparse punctate distribution of $InsP_3R$ was observed in a thin superficial layer similar to the distribution of functional release sites. For comparison, Fig. 8F (see color insert) shows $InsP_3Rs$ localized using conventional x–y scanning in fixed sections of the animal hemisphere of the oocyte. The more intense staining observed is likely due to a higher density of $InsP_3Rs$ in the animal hemisphere.[16]

A commercially available slide of multiply labeled endothelial cells (Fluo Cells, Molecular Probes) is shown in Fig. 8G (see color insert) as a readily available standard specimen allowing comparison with other CLSM systems. The image shows a pseudo-colored overlaid image of bovine artery endothelial cells imaged at 488ex./515em. to visualize fluorescein-labeled tubulin and 488ex./560em. to visualize Texas Red-labeled F-actin. A further example of resolution is shown in Fig. 8H: an x–y scan (488ex./515em) of a cultured primary cortical neuron stained with the lipid-soluble membrane dye Di8-ANNEPS (Molecular Probes) to visualize the surface membrane. Thin processes (<1 μm diameter) are resolved readily, and the apparent thickness of sections through the plasma membrane is 200–300 nm.

Conclusions

The objective of this article is to demonstrate the feasibility of constructing a custom confocal microscope that offers superior performance and versatility for dynamic Ca^{2+} imaging than commercial instruments at a fraction of the cost. No new principles are involved in our instrument and it is subject to the same theoretical limits of any confocal microscope; however, in practice, we have found its sensitivity and spatial resolution to exceed that of some commercial designs. The improvement probably lies in the simple optical design, the highly efficient detector, and that once having built the microscope the experimenter is well qualified to optimize and align the system. In our hands, this system has proved to be a versatile tool for the optophysiological study of many cellular processes, and construction of a similar instrument is well within the grasp of many investigators wishing to construct their own microscope "customized" to particular questions.

[16] N. Callamaras and I. Parker, *Cell Calcium* **15,** 66 (1994).

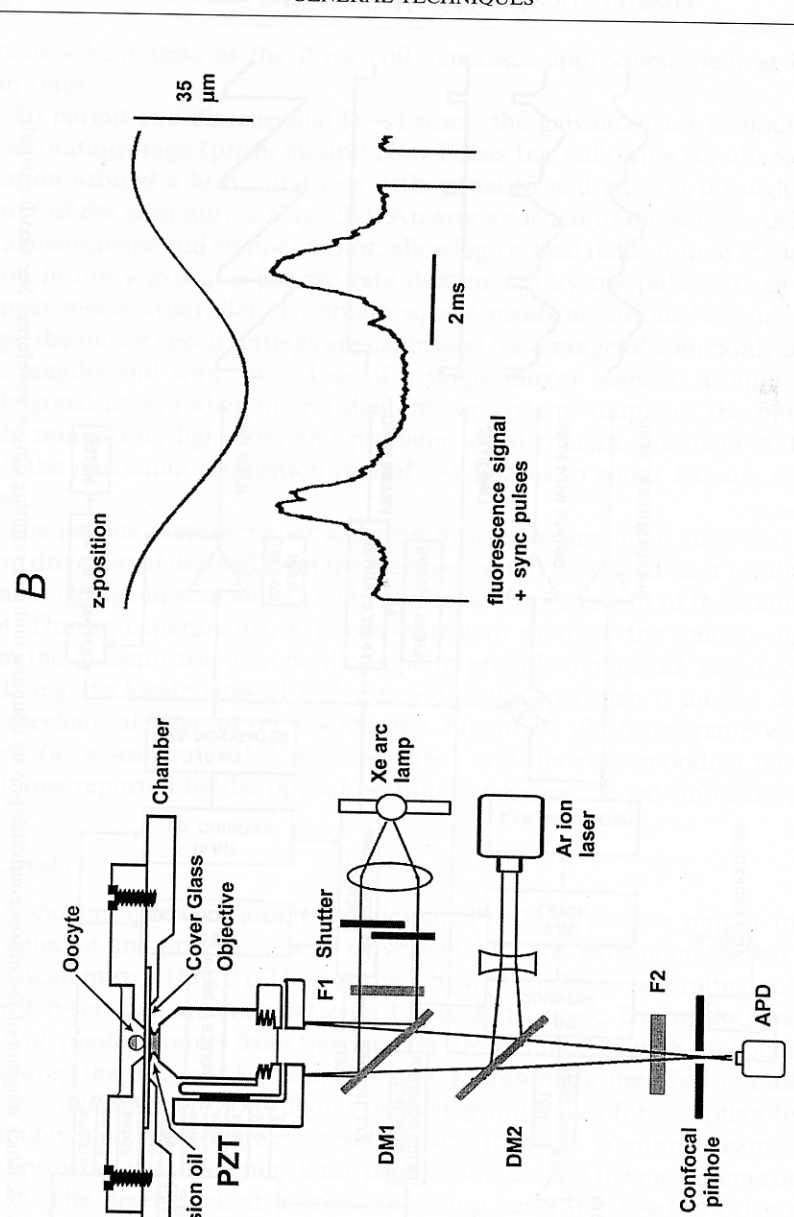
A
Oocyte
Chamber
Cover Glass
Objective
Immersion oil
PZT
F1
Shutter
Xe arc lamp
DM1
DM2
Ar ion laser
F2
Confocal pinhole
APD
B
z-position
35 µm
2ms
fluorescence signal + sync pulses